J. P. Soaphys, Vol 3, N°2 (2023) C23N22
http://dx.doi.org/10.46411/jpsoaphys.2023.016

Journal de physique de la SOAPHYS
http://www.soaphys.org/journal/
***ISSN Print :** 2630-0958*

An overview of Climate Change Impacts on the Health Sector for the Research Program of the National Adaptation Plan Support Project in Senegal

Diouf I.[1,*], Sy I.[2], Diouf D.[1], Ndione J.-A.[3], Gaye A.T.[1]

[1]Laboratoire de Physique de l'Atmosphère et de l'Océan-Siméon Fongang, Ecole Supérieure Polytechnique de l'Université Cheikh Anta Diop (UCAD), Dakar–Fann BP 5085, Senegal.
[2] Département de Géographie, Faculté des Lettres et Sciences Humaines (FLSH), Université Cheikh Anta Diop (UCAD) & Centre de Suivi Ecologique (CSE), Dakar, Sénégal
[3] Regional Agency for Agriculture and Food) 83 Rue des Patures (Super Taco), 01 BP 4817 – Lomé
* Corresponding author email: ibrahima23.diouf@ucad.edu.sn

INFOS SUR L'ARTICLE

Historique de l'article:
Reçu le : 04 aout 2022
Reçu en format revisé le : 10 septembre 2023
Accepté le : 10 octobre 2023

Keywords: Climate variability and Climate Change, Projections, Impacts, Health, diseases, Senegal.

RESUME/ABSTRACT

Senegal, a coastal country in the semi-arid Sahel region, faces significant risks associated with climate variability and climate change. Climate change is already affecting vulnerable people's wellbeing and it's expected to contribute to the (re)emergence of vector-borne, some water-borne and heat-related diseases, which will have disastrous consequences on the country's fragile health system and socio-economically vulnerable population. Our contribution to the National Adaptation Plan support Project - Global Environment Fund (NAP-GEF) aims to support community- based epidemiological surveillance and the design/maintenance of health information systems in order to improve planning, decision-making, and public health response. Our methodological approach aims to build a detailed climate and health database to describe the spatio-temporal characteristics of the climate-health relationships at national scale. Considering various indices of targeted diseases, we assess the degree of transmission of those diseases in Senegal for different historical period (1950-2014 and projections (2015-2100) based on a combination of the Shared Socio-Economic Pathways (SSPs) produced within the Coupled Model Intercomparison Project, phase 6 (CMIP6). Selected diseases include malaria, meningitis, dengue and Chronic – non communicable to heat waves. The project will strengthen institutional capacity to mainstream climate related risks within the Ministry of Health's strategies and governance model, enabling a public health system framework to support long-term and sustainable adaptation funding and programs. The project is being implemented jointly with the Ministry of Environment and Sustainable Development (MEDD) and the Ministry of Health and Social Action (MSAS). The findings in the project will guide and operationalize community-based early-warning systems and adaptation strategies specific to local climate-sensitive diseases in targeted regions in Senegal, which will feed into the national health prevention, response, and care strategies adapted to the needs of local communities. Development of scientific evidence and a knowledge management system get started in this study about the links between climate change and health through the launch of studies in collaboration with research institutions. However, barriers or limitations to integrating climate change data and information into health policies have also been identified.

INTRODUCTION

According to the World Health Organization (WHO), an increase in temperature and humidity and in variability of rainfall increases the risk of water-borne diseases through acceleration of availability and quality of larval sites, survival, persistence, transmission, and virulence of pathogens, shifts in geographical and seasonal distribution of diseases. Higher temperatures also contribute to higher risks of vector-borne diseases through the development of breeding sites accelerating parasite replication and survival of the adult Aedes and Anopheles, more frequent bites, and longer transmission seasons; a re-emergence of previously prevalent diseases; changes in the distribution and abundance of disease vectors and reduced effectiveness of vector. Winds also influence their movement, playing a favourable or unfavourable role in the dispersion of vectors depending on their direction and speed, and causing shift in the spatial distribution of diseases (Trape, 1999; Lidsay et al, 1996; Ndiaye et al, 2001). In addition, excessive heat increases the frequency and intensity of heatwaves which leads to higher rate of mortality due to excessive heat (Sy et al, 2022); increased incidence of heat stress and heat stroke, especially among those who work outdoor and the elderly; exacerbation of circulatory, cardiovascular, and respiratory; and increased premature mortality from ozone and fire-generated air pollution, especially during strong heat waves (Cissé et al, 2022; Trisos et al, 2022). Climate-induced health outcomes leads to Senegal's vulnerable communities, including children, women, and elders, facing increasing rates of morbidity and mortality, transferring national economic burden of health onto already highly vulnerable communities, and national health system, institutions and structures being vulnerable to climate hazards and disasters. Reduced health outcomes and increase of livelihoods insecurity leads to entrenched poverty among the Senegalese population and a possible decline in social development.

In Senegal, according to the Minister of Health and Social Action of Senegal MSAS (2019), the health status of the Senegalese population is marked by the persistence of the burden of climate sensitive diseases including malaria, dengue, meningitis, and climate-sensitive and non-communicable diseases such as respiratory diseases and cardiovascular diseases.

Regarding malaria, it is a vector-borne disease whose existence and transmission depend on three main factors: the plasmodium parasite, the Anopheles vector, and the human host. Beyond these essential factors, the risk of malaria transmission can be maintained or reinforced by environmental conditions, or climatic conditions as well as socio-economic factors. In particular, the transmission of malaria is very sensitive to climate and atmospheric conditions. When these are unusual, for example during heavy rainfall, mosquito populations can multiply and trigger epidemics. We have previously studied the climate-malaria relationship (e.g., in Diouf et al., 2017) as well as the predictability of high malaria occurrences in Senegal and West Africa more generally (Diouf et al. 2021). With these studies, we have already noted a causal relationship between El Niño and malaria parameters. These results were endorsed in Diouf et al. 2021b by coupling the LMM malaria model (Liverpool Malaria Model) of Hoshen et al., 2014 and the S4CAST (SST-based statistical ForeCAST) of Suárez-Moreno and Rodríguez-Fonseca, 2015.

Moreover, several other vector-borne diseases, including dengue fever, are very sensitive to climatic and meteorological conditions. Dengue is one of the major public health problems, and it is a major cause of hospitalization and death, especially for children in endemic countries (Bhatt et al., 2013; Brady et al., 2012). Dengue fever is a vector-borne disease whose presence and transmission depend on three essential factors: the host, the pathogen, and the mosquito vectors (including Aedes. aegypti). In addition to socioeconomic factors, including population growth, lack of sanitation, increased human movement, and ineffective mosquito control, the risk of dengue transmission may be maintained or increased by environmental or climatic conditions. The effect of climatic parameters will be of particular interest in this study. Previous studies have shown that climatic factors contribute to global changes in dengue incidence and distribution. Although numerous studies have been carried out on the relationship between climatic conditions and dengue fever transmission, the effects of climate parameters on this vector-borne disease remain largely unexplored in our study area (West Africa and Senegal). notably). We attempt to identify and better describe the climate impact on observed dengue data and assess the capability of climate-based dengue models. Climate information from the latest climatological period will be used to drive existing statistical and process-based models to refine our knowledge of the relationships between climate and dengue fever. These biological statistical models will be driven by the Modeling Coupled Model Intercomparison Project, Phase 6 CMIP6 (Eyring et al., 2016).

For Meningitis, it appears in waves of epidemics and is one of the diseases that kill the most in West Africa. It generally affects children from 0 to less than 15 years old and sometimes adults. Since then, it has become a public health problem, hence the need to know and understand the risk factors allowing its appearance and its spread. Thus, recent studies at the end of the AMMA program (Multidisciplinary Analysis of the African Monsoon) have established a correlation between the episodes of dust observed during the dry season and the outbreak of meningitis epidemics (Jeanne et al., 2005; Martin and Chiapello, 2013). Therefore, climate variability is one of the risk factors for meningitis epidemics. However, since this link between climate and meningitis is not well documented in Senegal, or even in Africa, drawing inspiration from work on climate-health links in Senegal, including, among others, Ndione et al., 2008 on the rift valley fever and Diouf et al. (2017, 2020), on malaria, we in turn exploited certain climatic variables on a spatio-temporal scale. The relationship between meteorological/dust variables and the number of meningitis cases in Senegal is studied with pre-existing meningitis models.

In addition, most scientists agree on the existence of a global warming phenomenon that will increase the frequency and intensity of heat waves in all regions of the world. On the one hand, periods of high heat are associated with morbidity and mortality problems, particularly in people with sensitive respiratory or cardiovascular diseases. Heat stress has direct and indirect health effects. Among the most marked direct effects are exhaustion and heat stroke. Indirect effects, which affect many more people, usually result from the exacerbation of a chronic condition, such as cardiovascular and respiratory conditions. In temperate regions, very high temperatures during generally milder periods are associated with increased mortality. The phenomenon is less constant in the tropics, where temperatures are high for long periods and also vary less. On the other hand, in countries with marked temperature variations, the mortality rate rises in winter, when respiratory and infectious diseases are on the rise. A low temperature increases blood pressure and the efforts of the heart. People with heart problems are more at risk and should avoid overworking themselves. Colds also reduce resistance to infections, from the common cold to more serious illnesses, such as the flu. Low humidity during the winter months dries out the skin and can cause dermatitis (inflammation of the skin). As the cold reduces blood circulation by constricting the vessels, it can also damage the tissues and cause frostbite (damage to the skin by the cold).

This work is organized as follows: Section 2 presents the different types of data used and the methods applied. Section 3 studies the spatio-temporal simulated diseases' indices various climate and atmospheric. Finally, a summary and discussion of the main results are provided in Section 4.

DATA AND METHODS

I.1. Data

II.1.1. Health observations data used in this study

In terms of observation, we acquired health data from health districts, from MSAS sentinel sites. Senegal's health

data are often structured according to the flowchart in figure 1 giving an overall view of the disaggregation of the MSAS database, even if this organization does not have a long enough time series for the needs of this study. The health data obtained so far contains the number of cases of the disease recorded on an annual scale and by region. The health databases (Table 1) were made available to us by the DGS (Direction Générale de la Santé). However, even though other diseases including Rift Valley Fever (RVF) are priority diseases in this study, we were unable to obtain observational data.

Table 1: Health data used.

Disease	Period	Spatial scale	temporal scale	Indicators
Malaria	2011-2021	To study the spatial distribution of diseases at the national level, data is collected for the 14 regions of Senegal	Données mensuelles	Number of confirmed cases of the disease
Meningitis				
Dengue				
Severe Diarrhea				

I.2. Climate data

In this study, we have used climate data from the WFDEI as reference data (Dee et al., 2011) and the multi-model ensemble mean of fifteen (15) global circulation models, for instance, Coupled Model Intercomparison Project, version 6, where bias correction technique, the CDF-t (Cumulative Distribution Function transform) method (Michelangeli et al., 2009), was applied. The WATCH Forcing Data methodology applied to ERA-Interim data (WFDEI), Weedon et al., 2014, is produced from Watch Forcing Data (WFD) and ERA-Interim reanalyses via sequential interpolation at 0.5° resolution, an altitude correction and monthly scale adjustments based on monthly observational data from CRU (Climate Research Unit) TS3.1/TS3.21 and GPCCv5/v6. Details of the three products can be found in Dee et al., 2011 for ERA-Interim and Weedon et al., 2014 for WFDEI. The variables have a daily time step with a spatial resolution of 0.75° (~80 km) and 0.50° (~55 km) respectively for ERA-Interim and WFDEI, being qualified as low resolution and medium resolution. For the heat indices calculation, knowing that the required variables such relative humidity are not available in our WFDEI database, we alternatively use the ERA5 data (the European Re-Analysis, 5 th Generation). ERA5 (Hersbach et al. al, 2020) is a climate reanalysis dataset developed by the European Centre for Medium-Range Weather Forecasts (ECMWF). It provides a comprehensive and consistent global view of the Earth's atmosphere, land surface, and oceans over the past few decades, based on historical observations and atmospheric models. ERA5 incorporates a wide range of variables, such as temperature, humidity, wind, precipitation, and pressure, with high spatiotemporal resolution. It is widely used in climate research and provides valuable information for studying past climate conditions and understanding climate variability and change.

In addition, for the meningitis study with respect to atmospheric parameters, we use the Aerosol Optical Depht (AOD) from the AERONET (AErosol RObotic NETwork) website https://aeronet.gsfc.nasa.gov/.

Moreover, about ten global climate models from CMIP6 (Coupled Model Intercomparison Project, version 6) for the precipitation and temperature variables are used. These simulations are available in daily time steps for the period 1850-2014 (Historical) and 2015-2100 (projections). The available models are shown in Table 2. They are available at different spatial resolutions which, for example, ranges from 100 km (EC-Earth3) to more than 350 km (CanESM5). The data sets (observed and simulated) used were interpolated on the grid finally to make them consistent in the analysis and interpolation. The period 1985 to 2014 was chosen as the reference period.

Table 2: CMIP6 models, their institutions and countries of origin, and their resolution.

Model name	Institution and country	Spatial resolution (Latitude x Longitude)
ACCESS-CM2	Australian Community Climate and Earth System Simulator Climate Model Version 2	1.9° x1.3°
ACCESS-ESM1-5	Australian Community Climate and Earth System Simulator Earth System Model Version 1.5	1.9°x1.3°
BCC-CSM2-MR	Beijing Climate Center (BCC) and China Meteorological Administration (CMA), Chine	1.1 x1.1
BCC-ESM1	Beijing Climate Center (BCC) and China Meteorological Administration (CMA), Chine	2.81° × 2.81°
CanESM5	Canadian Earth System Model, Canada	2.81° × 2.81°
CESM2	National Center for Atmospheric Research, Climate and Global Dynamics Laboratory, USA	1.25° × 0.94°
CESM2-WACCM	National Center for Atmospheric Research	1.25° × 0.94°
CMCC-CM2-SR5	The Euro-Mediterranean Center on Climate Change, Italie	2.8° x 1.9°
CNRM-CM6	Centre National de Recherches Météorologiques-Centre Européen de Recherches et de Formation Avancée en Calcul Scientifique, France	1.4° x 1.4°
CNRM-CM6_HR	Centre National de Recherches Météorologiques-Centre Européen de Recherches et de Formation Avancée en Calcul Scientifique, France	0.5° x 0.5°
CNRM-ESM2-1	Centre National de Recherches Météorologiques-Centre Européen de Recherches et de Formation Avancée en Calcul Scientifique, France	1.4 ° × 1.4°
EC-Earth3	EC-EARTH Consortium (27 institutions), Europe	0.70 ° × 0.70°
EC-Earth3-Veg	EC-EARTH Consortium (27 institutions), Europe	0.70 ° × 0.70°
FGOALS-g3	Flexible Global Ocean-Atmosphere-Land System model Grid-point version 3	2° x 2.3°
GFDL-CM4	Geophysical Fluid Dynamics Laboratory, USA	2.50 ° × 2.00°
GFDL-ESM4	Geophysical Fluid Dynamics Laboratory, SUA	1.25 ° × 1.00°
IITM-ESM	Indian Institute or Tropical Meteorology, India	1.9 ° x 1.9°
INM-CM4-8	Numerical Mathematics, Russian Academy of Science, Moscow 119991, Russie	2° x 1.5°
INM-CM5-0	Numerical Mathematics, Russian Academy of Science, Moscow 119991, Russie	2° x 1.5°
IPSL-CM6A-LR	Institut Pierre-Simon Laplace, France	2.5° x 1.3°
KACE-1-0-G	National Institute of Meteorological Sciences, Korea	1.4° x 1.9°
KIOST-ESM	Korea Institute of Ocean Science and Technology, Korea	1.875° x 1.875°
MIROC6	Japan Agency for Marine-Earth Science and Technology, Kanagawa 236-0001, Japan	1.4° x 1.4°
MIROC-ES2L	Japan Agency for Marine-Earth Science and Technology, Kanagawa 236-0001, Japon	2.8° x 2.8°
MPI-ESM1-2-HR	Max Planck Institute for Meteorology, High Resolution, Allemangne	0.9° x 0.9°
MPI-ESM1-2-LR	Max Planck Institute for Meteorology, Low Resolution, Allemangne	1.9° x 1.9°
MRI-ESM2	Meteorological Research Institute, Japon	1.1° x 1.1°
NESM3	Nanjing University of Information Science and Technology, Nanjing,	1.9° x 1.9
NorESM2-LM	Norwegian Meteorological Institute Low Medium Norway	2.5° x 1.9°
NorESM2-MM	Norwegian Meteorological Institute Medium Medium Norway	0.9° x 1.3°
TaiESM	Research Center for Environmental Changes, Taiwan	1.3° x 1°

To study potential future impacts, the IPCC (Intergovernmental Panel on Climate Change) in its 6th report (Zhongming et al., 2021) relies on scenarios called Shared Socio-economic Pathways (SSP) or "economic trajectories". Economists and sociologists assess the costs of adaptation and mitigation related to climate change according to different socio-economic scenarios compatible with Representative Concentration Pathway (RCP) scenarios. RCP scenarios are four scenarios of radiative forcing pathways until the year 2100. These scenarios were established by the Intergovernmental Panel on Climate Change (IPCC) for its 5th Assessment Report, AR5. An RCP scenario is used to model future climate. In the IPCC's Fifth Assessment Report (AR5, published in 2014) and based on four different assumptions regarding the quantification of greenhouse gases to be emitted in the coming years (2000-2100), each RCP scenario provides a likely variant of the climate resulting from the chosen

emission level assumption. The four scenarios are named after the resulting radiative forcing range for the year 2100: RCP 2.6 corresponds to a forcing of +2.6 W/m² (Watt per square meter), RCP 4.5 corresponds to +4.5 W/m², and similarly for RCP6 and RCP8.5. The higher this value, the more energy the Earth-atmosphere system gains and warms up. These scenarios, called SSPs, are presented in terms of the efforts required for adaptation and mitigation if the world follows such scenarios. The latest generation of CMIP, IPCC-AR6 (December 2021), includes 31 modeling groups.
In this study, we particularly focus on three climate change scenarios in CMIP6: the optimistic scenario (ssp126), the moderate scenario (ssp245), and the extreme or pessimistic scenario (ssp585) (Table 3).

Table 3: CMIP6 Data, Scenarios, and Time Scales

Simulations	Scenarios	Available period	Selected Period
Climatological reference		1850-2014	1985-2014
Projections	ssp126 ssp245 ssp585	2015-2100	2015-2080

II.3. METHODS

II.3.1. The malaria model

The LMM (Liverpool Malaria Model) is a dynamic model of malaria based on daily time series of rainfall and temperature. The different components of the malaria transmission model and the calibration of the parameters are described in more detail by Hoshen and Morse (2004) then Ermert (2011). The LMM is a mathematical-biological model of parasite dynamics, which includes intra-vector phase dependent on metrological conditions and phase within the host independent of metrological conditions. The mosquito population is simulated using larval and adult stages, the number of eggs deposited in the breeding sites and the larval mortality rate according to the rains of the previous 10 days. The mortality rate of adult mosquitoes and the egg-laying/biting cycle (called the gonotrophic cycle) depend on temperature. The process of parasite transmission between humans and mosquitoes is modelled with a temperature dependence for the parasite reproduction rate (sporogonic cycle) and mosquito biting rate. The two cycles evolve based on the number of "degree-days" above a certain temperature threshold. Respectively, the gonotrophic and sporogonic cycles take about 37 degree-days and 111 degree-days with a threshold of 9°C (18°C) (Caminade et al., 2011). Climate and health studies have used LMM simulations in southern Africa, including Zimbabwe, Botswana and across the African continent (Morse et al., 2005; Jones et al., 2010). The output variables of the model are, among others, the incidence, prevalence, mosquito population, etc. The current version of the model (LMM2010) has shown significant improvements in the simulation of malaria dynamics in sub-Saharan African countries including Senegal. This version has also been used by [48-50] to assess the risk posed by future climate change on malaria, including Senegal with the work of Diouf et al. (2013; 2017; 2020).

II.3.2 Poisson regression modeling applied to meningitis

Poisson regression is a useful tool for analysing incidence rates in studies of cohorts or groups of individuals (number of events related to a number of person-years of exposure). It is also useful for comparing event counts (such as the average number of events for a patient over a follow-up period). What is less well known is that the use of Poisson regression facilitates time trend analyses of baseline risks, relative or absolute excess risks, and other aspects of risk functions that can be difficult to assess with other methods. The Kaplan-Meier method, the logrank test and the Cox model each have their respective parallel in the analysis of grouped data: instantaneous risks, relative risks on grouped data and Poisson regression grouped by intervals. This approach makes it possible to present the instantaneous speed of occurrence of events, which is potentially more meaningful for clinicians, and to consider certain constraints more easily. Indeed, for example, this approach facilitates the consideration of time-dependent variables, a time-dependent effect, competing risk or interval exposure or in the calculation of excess mortality.

II.3.3. Dengue fever relative vectorial capacity (rVc) model.

An rVc model describes the ability of a vector to spread disease among humans and takes into account host, virus, and vector interactions (Garrett-Jones, 1964; Liu-Helmersso, 2012) assuming that these three parameters are present. It represents the average daily number of secondary cases generated by a primary case introduced into a fully susceptible population (Garrett-Jones, 1964). From the classical definition of Anderso et May, 1991, the rVc model can be expressed as follows:
$rVc= \alpha^2 \beta_h\beta_m e^{-\mu_m{}^n})/\mu_m$; where:

- 1) α =*Biting rate* (Scott et al., 2000);
- 2) β_m = *probability of infection from humans to vector per bite* (Lambrechts et al., 2011);
- 3) β_h = probability *of transmission from vector to human per bite* (Lambrechts et al., 2011; Scott et al., 2000) ;
- *4) η = Extrinsic incubation period* (Focks et al., 1995; Watts et al., 1987; McLean et al., 1974) ;
- 5) μ_m = Mortality *rate* (Yang et al., 2009).

The equations of these five parameters are respectively given below:

1) ***Biting rate (α)***
$\alpha(T)=0.0043T+0.0943$ for $21°C \leq T <= 32°C$

2) ***The probability of infection from humans to vector per bite (βm)***

$(\beta m) = 0.0729T-0.9037$ for $12.4°C <= T \leq 26.1°C$
$(\beta m) = 1$ for $26.1°C < T < 32.5°C$

3) ***The probability of transmission from vector to human per bite (βh)***

$(\beta h)=0.001044T(T-12.286)(32.4461-T)^{1/2}$ for $12.286°C \leq T \leq 32.461°C$

4) ***Extrinsic incubation period (η)***

$\eta\ (T)=4+e^{5.15-0.123T}$ for $12°C \leq T \leq 36°C$

5) Mortality rate (μ_m)

$\mu_m(T)=0.8692-0.1590T+0.01116T^2-3.408x10^{(4)}T^3+3.809x10^{-6}xT^4$ for $10.54°C \leq T \leq 33.41°C$

II.4. Heat calculation Heat Wave Index

The heat and discomfort index calculation are applied to the multi-model ensemble mean of CMIP6 projections as part of the study of future changes in heat stress and risk regions under global warming scenarios at different time scales in Senegal. To assess the stress induced by the combined effects of temperature and humidity, we applied the NOAA (National Oceanic and Atmospheric Administration) NWS (National Weather Service) heat index formulation (hereafter referred to as HI) developed by Rothfusz (1990), which is given by the following equation:

$$[hi,confort] = heat\_index(Tf,RH);$$
$$HI=-42.379 + 2.04901523*T + 10.14333127*RH - 0.2247554T*RH-6.8378*10^{-3*}T^2 – 5.48172*10^{-2}*RH^2 + 1.229*10^{-3}T^2*RH + 8.528*10^{-4}T*RH^2 – 1.99*10^{-6}*T^2*RH^2$$

where T is the temperature in degrees Fahrenheit (°F) and RH is the relative humidity in percent. This formulation was developed through multiple regression analysis of Steadman's (1979) equation for apparent temperature (which considers many physiological and environmental factors) to adopt two commonly used and conventional variables (i.e., ambient air temperature and relative humidity). HI is therefore the heat index expressed in apparent temperature in degrees Fahrenheit.

This full regression equation is only appropriate when the temperature and humidity values generate an HI greater than 80°F (i.e., 27°C). In this case, a number of adjustments are applied to this formula depending on the temperature and relative humidity values.

First, if RH is less than 13% and T is between 80°F and 112°F, the following adjustment is subtracted from HI:

ADJUSTMENT = $((13-RH)/4)*((17-abs(T-95))/17)^{1/2}$;

Second, if RH is greater than 85% and T is between 80°F and 87°F, the following adjustment is added to HI:

ADJUSTMENT = ((RH-85)/10)*((87-T)/5) ;

This function calculates the heat index from the temperature in degrees Fahrenheit and relative humidity. The heat index is given in Fahrenheit and comfort is given in 4 classes: "uncomfortable" =1; “extreme discomfort” =2; "hazard"=3; "extreme danger"=4.

Within the framework of modeling, using various indices of priority diseases selected during the project's launch workshop, we assess the level of transmission of these diseases in Senegal using different tools/approaches (Table 4).

Table 4: Priority Diseases and Tools/Approaches

Diseases			Impact model or Tool
Communicable diseases	Vector-borne diseases	Malaria	Liverpool Malaria Model (LMM)
		Dengue	relative vectorial capacity (rVc) model of dengue
	Airborne diseases	Meningitis	Poisson regression model
Non-communicable diseases	Chronic diseases (Cardiovascular diseases, Respiratory diseases, kidney diseases, Neurological diseases, Metabolic diseases)		Comfort index

RESULTS AND DISCUSSION

III.1 Mapping of observed diseases over Senegal (2011-2021)

The spatial distribution of different recorded diseases between 2011 and 2021 in Senegal is illustrated in figure 1. These figures represent the spatial variations of malaria, dengue, meningitis, and severe diarrhea (bloody diarrhea) in Senegal, respectively. The southern and southeastern parts are heavily affected by malaria (figure 1a). For dengue (figure 1b), the northwest (Saint-Louis) and the central-western part of the country (particularly Diourbel) are the most affected areas. Meningitis (figure 1c) is prevalent in the central and southern parts of the country, as well as in the west, specifically in Dakar. The high number of cases of diseases could also be linked to the regularity of data collection. Severe diarrhea (or bloody diarrhea) is mainly observed in the eastern part of the country but also in the central-western region (Dakar, Thies, and Diourbel). In particular, the high occurrence of certain diseases in regions like Dakar, despite unfavorable climatic conditions, can be explained by the fact that it is in Dakar where people have more of a culture of seeking medical diagnosis and treatment, resulting in more regular data collection. This is the case for meningitis, as hospitalizations for meningococcal meningitis at Fann Hospital (Dakar) are partly due to its status as a national pediatric reference center. As such, it receives most children from the Dakar region and occasionally from other parts of Senegal. However, for modeling purposes, only climatic factors are considered, and the impact models do not consider socio-economic parameters as in the case of observations.

Table 5 provides a summary of the climate-sensitive diseases included in the study and the most vulnerable regions considering the climatic parameters influencing the presence and/or development of each disease.

Table 5: Priority climate-sensitive diseases

Disease	Climatic parameters	Regions or most affected areas
Malaria	Rainfall, temperature, humidity, and wind	**Southern and Southeastern Regions**: Ziguinchor, Sédhiou, Kolda, and Kédougou **Central Regions:** Kaolack, Kaffrine, Fatick, Diourbel, Thiès, and Dakar
Meningitis	Temperature, humidity, wind, and dust	**Northern and Northwestern Regions:** Matam, Louga, and Saint-Louis **Central Regions:** Dakar, Thiès, and Diourbel
Dengue	Rainfall, temperature, humidity	**Northern and Northwestern Regions:** Matam, Louga, and Saint-Louis **Eastern Regions:** Tambacounda and Kédougou
Diarrheal diseases	Rainfall, temperature	**Northern Regions:** Matam **Central Regions:** Kaffrine, Tambacounda, Thiès, Dakar, and Diourbel
Non-communicable diseases sensitive to heatwaves	Temperature, humidity, wind, and solar radiation	**Northern Regions:** Matam, Louga **East and Southeast:** Tambacounda and Kédougou

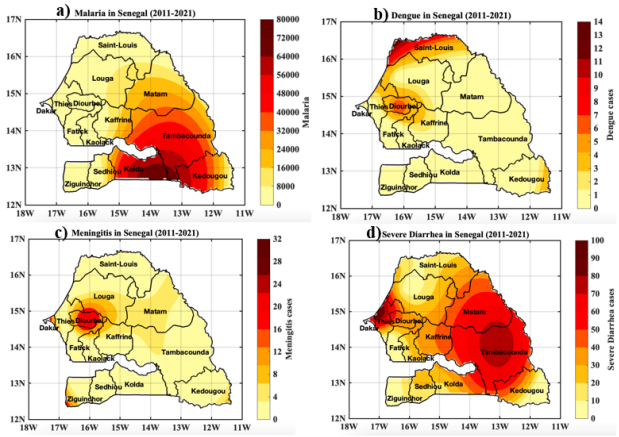

Fig. 1: Spatio distribution of climate-sensitive diseases in Senegal between 2011-2021: a) Malaria, b) Dengue, c) Meningitis, and g and d) Severe diarrhea.

I.3. Malaria

In figure 2, we analyse the spatio-temporal variability of malaria incidence simulated by the LMM model forced by daily precipitation and temperature data. We illustrate the spatio-temporal distribution of malaria in Senegal corresponding to that obtained previously with rainfall and temperature at WFDEI in Senegal. In terms of spatial variability, there is a clear difference in the intensity of the malaria incidence signal between the northern and southern regions of Senegal. A very intense signal is observed in the southern part of Senegal, while in the far north, the signal is very weak. Indeed, the strong occurrence only extends around 15 ºN. However, the important transmission occupies practically the whole country with of course maximum values between 11 ºN and 15 ºN. A particularly high signal is observed for the incidence during the September-October-November season with a maximum in October. Knowing that the LMM model only takes precipitation and temperature into account, this very intense signal should be explained by extreme values of rainfall and/or temperature recorded locally.

The seasonal cycle of the simulated incidence of malaria is represented in figure 3. The analysis of the seasonal evolution shows an incidence rate close to zero during the months of January to June. From June, we see an increase in incidence which reaches the maximum median peak in October with a rate of more than 60%. Malaria transmission follows the rhythm of rainfall. The rainy season is the period of high mosquito density. Other studies have shown that the peak of malaria mostly follows the peak of rainfall. Thus, the season of high malaria transmission has a maximum shifted by one to two months compared to that of precipitation. The lag between the peaks of rain and the incidence of malaria is explained by the fact that intermittent rains (or showers too) in August can on the one hand reinforce the development of the population of mosquito vectors triggered at the onset of the first rains, but these heavy rains in August largely drown the eggs deposited on surface waters by female mosquitoes. In addition, the low temperatures generated by the succession of rainy days are not favorable to the rapid growth of vectors, from larvae to infectious mature mosquitoes through the nymph stage. On the other hand, with a delay of 1 to 2 months, the mosquito vectors saw their living conditions improved with the wastewater, the strong heat of this still humid month (humidity increases the longevity of mosquitoes), to this add environmental conditions with the availability of large breeding places and vegetation cover that constitute mosquito nests. This delay is quite logical in relation to what is known of the biology of the Anopheles vector and of the sporogonic cycle of the plasmodium parasite.

Figures 4a and 4b illustrate consistency between the malaria incidence simulated by the LMM model forced by the WFDEI (reference data) and that obtained from the CMIP6 data, both with the historical and with the different scenarios. For the spatial variability, there is still a clear difference in the intensity of the signal of the malaria incidence between the northern regions and the southern of Senegal. The latitudinal gradient of the distribution of malaria in Senegal would be still maintained. By comparing with historical data (figures 3a and 3b), we find that the simulated malaria incidence decrease likely tends to prevail over many portions of Senegal, in the north and the centre, and this, even in the near future (2015- 2044), but especially in the far future (2050-2080). The magnitude of the decrease is more important with the ssp245 and ssp585 scenarios (figures 3d, 3e, 3g, and 3h). Such a decrease in malaria in the far future appears to be associated with climate change (Gething et al. 2010; Beguin et al. 2011; Diouf et al., 2021). Thus, temperatures that are too hot could have a negative impact on the adult mosquitoes' survival by starting to reduce the population of adult mosquitoes in the model and this implies a decrease in malaria transmission. Beguin et al., 2011 showed an opposite effect of climate change on the global distribution of malaria, and they show a decrease in simulated malaria behaviours over the Sahel regardless of the period and scenario considered which are related to temperature effect. However, looking at the southern part of Senegal in figures 3c and 3f and comparing with figure 4a as a point of reference, malaria is expected to increase in the southern part of the study area. This agrees with the results of previous studies on West Africa such as Peterson (2009) who showed that the epidemic fringe would be shifted to the south for most of malaria models. It is expected that during the 2080s, the climate will become so unsuitable in the northern part of the Sahel including the northern regions of Senegal, without more people at risk (Caminade et al. 2014).

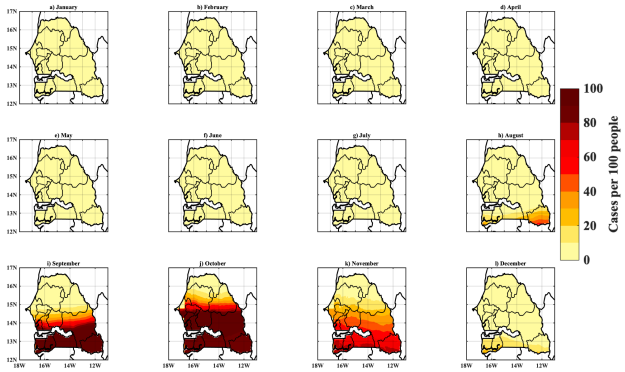

Fig.2. Spatial distribution and seasonal evolution of malaria incidence for the period 1979-2018: LMM model simulations based on WFDEI data.

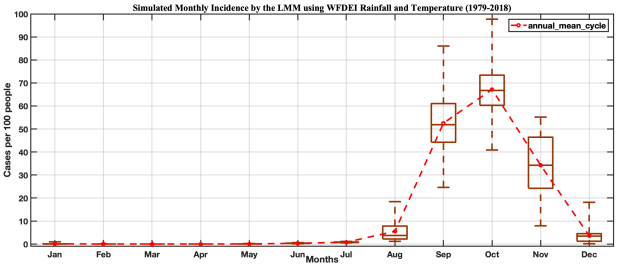

Fig.3. Intra-annual variation in incidence for the period 1979-2018: LMM model simulations based on WFDEI data.

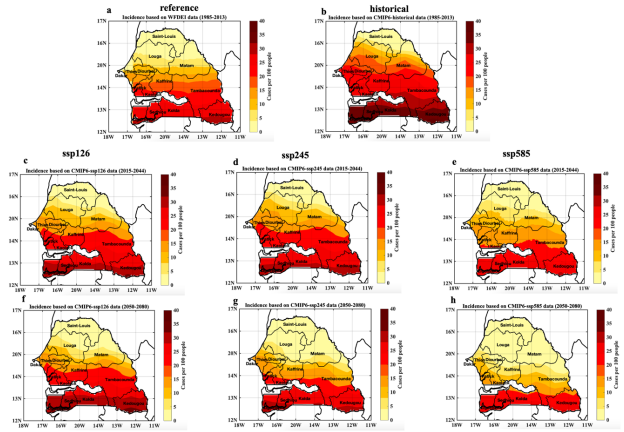

Fig.4. Spatial distribution of malaria incidence: a) for the historical period 1985-2013 and for simulations using WFDEI data as reference, b) for the historical period 1985-2013 and for simulations using CMIP6 data, e-h) for the 2015-2080 projections and for the simulations based on data respectively from scenarios SSP126, SSP245, SSP585 of the CMIP6.

I.4. Dengue

Figure 5a shows that the North-East, notably a good part of Saint-Louis, Matam and Louga, the East of the country, i.e., Tambacounda and certain parts of the central regions, are the most affected by the high occurrence of the rVc index of dengue fever. As seen before with another vector-borne disease such as malaria, figures 5b, 5c and 5d relating to dengue projections show an opposite effect of climate change on the future distribution of dengue in Senegal. For example, figure 5d (extreme scenario ssp585) shows a drastic decrease in the simulated index (rVc) of dengue in eastern Senegal, which is also observed but to a lesser extent with the optimistic scenarios (ssp126, figure 5b) and medium (ssp245, figure 4c). This result on the future reduction of dengue fever in certain regions of the country is linked to an effect of extremely hot temperature. Thus, too hot temperatures could have an impact on the survival pattern of adult mosquitoes starting to kill many adult mosquitoes in impact models and this implies a decrease in the transmission of certain vector-borne diseases such as malaria and dengue fever. However, figures 4a and 4c show that dengue fever is expected to spread in southern Senegal in the long term in Ziguinchor and Sedhiou.

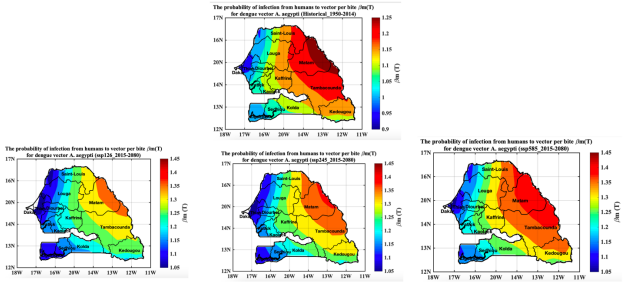

Fig.5. Spatial distribution of rVc (relative vectorial capacity) in Senegal: a) historical period (1950-2014), and projections (2015-2080), b) sssp126 scenario, c) ssp245 scenario and d) ssp585 scenario.

I.5. Meningitis

In figure 6a, using the daily averaged surface weather variables (zonal wind at 10m, southerly wind at 10m and relative humidity and temperatures at 2m) from the European Center for Medium-Range Weather Forecasting (ECMWF) which are ERA-Interim data (Dee et al., 2011) are used, as well as satellite products of in situ data (see Table in the July activity report). There is a high concentration of the number of meningitis cases when the temperature is high, with a temperature range between 25°C and 30°C. The high concentration of the number of meningitis cases corresponds to a low relative humidity rate, between 20% and 40% (figure 6b). In general, low humidity is a necessary and not sufficient condition for the onset and evolution of the meningitis season, on the other hand, high humidity (arrival of the monsoon) is a sufficient condition to stop the transmission. On the other hand, the concentration of the number of meningitis cases corresponding to a high AOD was expected, which is not the case in figure 6c. We note that the temperature is high there (about 32°C), the humidity less than 30% and the negative southerly wind or harmattan (figure 6d).

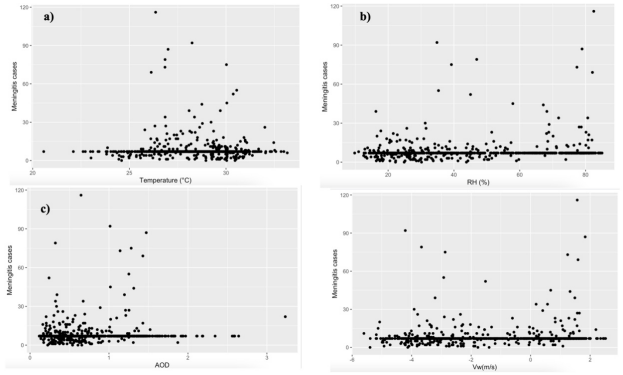

Fig.6. Relationship between the number of cases of meningitis and climatic parameters (2006-2020): a) temperature, b) relative humidity and c) AOD.

The histograms of the health climate variables (temperature, relative humidity, AOD and cases of meningitis) are given in the 1st column of figure 7. These histograms give an overview of the distribution of each variable. They show a significant variability of the observations, which requires a transformation of the series by applying the logarithm (2nd column figure 7). The log function applied to the data decreases the variability between observations. The application of the log makes it possible to have a histogram which resembles that of the observations generated by a normal law mechanism, or Gauss's law, where the probability density gives a bell-shaped curve symmetrical with respect to the axis of the ordered. Knowing that the variability of our data or the variance is very large, it is recommended to work with the transformed data (by log application).

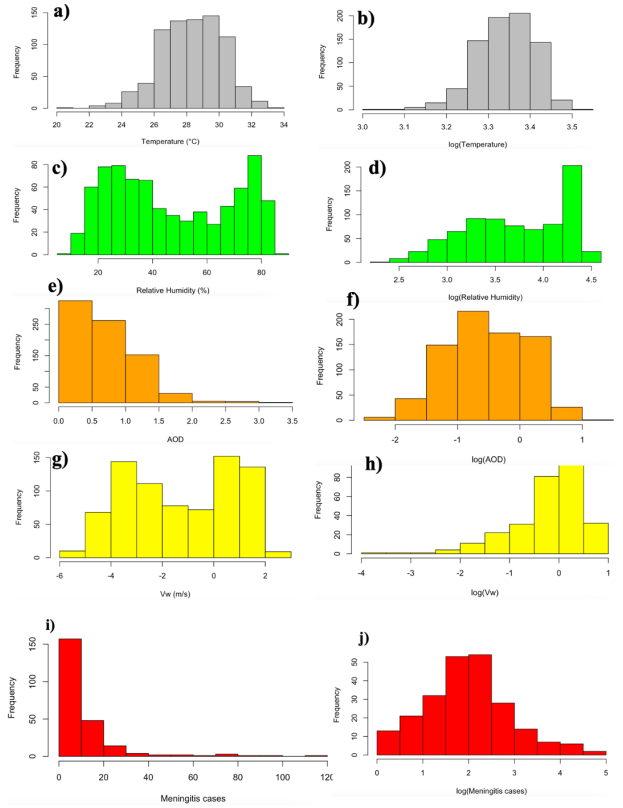

Fig.7. Histograms of climate and health variables (2006-2020). 1st column (a, c, e, and i): temperature, relative humidity and AOD and number of cases of meningitis respectively, and 2nd column: Histograms of the variables after transformation of the series by application of log.

I.6. Chronic – non communicable diseases to heat waves.

Heatwaves can exacerbate the effects of climate-sensitive non-communicable diseases (NCDs), which are chronic illnesses whose incidence or severity can be influenced by the climate. Here are some examples of NCDs that can be aggravated by heatwaves:

• Cardiovascular diseases: Heatwaves can exert additional stress on the cardiovascular system. High temperatures can increase heart rate, blood pressure, and blood viscosity, which can worsen symptoms of pre-existing heart conditions such as angina and heart attacks.

• Respiratory diseases: Individuals with respiratory diseases such as asthma and chronic obstructive pulmonary disease (COPD) may experience increased breathing difficulties during heatwaves. High temperatures can worsen airway inflammation and increase the risk of respiratory crises.

• Kidney diseases: Individuals with kidney diseases, including chronic kidney failure, may be more vulnerable to heatwaves due to reduced ability to regulate body temperature and eliminate metabolic waste. High temperatures can worsen dehydration and stress on the kidneys.

• Neurological diseases: Individuals with neurological diseases such as Parkinson's disease and multiple sclerosis may be heat-sensitive. Heatwaves can worsen neurological symptoms such as fatigue, muscle weakness, and coordination problems.

• Metabolic diseases: Individuals with metabolic diseases, including diabetes, may be more vulnerable to heatwaves due to increased difficulties in regulating blood sugar levels. High temperatures can increase insulin resistance and the risk of metabolic complications.

It is important for individuals with climate sensitive NCDs to take precautions during heatwaves, such as staying hydrated, avoiding outdoor activities during the hottest hours of the day, wearing lightweight clothing, and seeking cool environments. Additionally, healthcare systems and health authorities should be prepared to handle increased healthcare needs during periods of extreme heat to provide adequate support to vulnerable individuals with NCDs.

In figure 8, categories of comfort index or thermal stress are represented using temperature and humidity data from ERA5 to calculate the heat index before deducing these comfort index categories. The Comfort Index (CI) is a measure used to assess the comfort level experienced by individuals in a specific environment, typically related to weather or thermal conditions. It is often calculated based on factors such as air temperature, relative humidity, wind speed, and sometimes other variables like radiant temperature. The Comfort Index helps to gauge how comfortable or uncomfortable a given climate or weather condition is for human beings. It is especially relevant in assessing thermal comfort, which refers to the level of

satisfaction a person experiences in terms of their body temperature in relation to the surrounding environment. Various Comfort Index scales exist, and they are designed to categorize the comfort level into different ranges, such as comfortable (or safe), uncomfortable (caution), extreme discomfort (or extreme caution), and dangerous conditions (or danger). These scales can be used to interpret the Comfort Index values and provide information about the potential health risks associated with certain weather conditions. Figures 8a-d represent the CI for the four seasons, namely December-January (DJF), March-May (MAM), June-August (JJA), and September-November (SON). In Figure 8a, it is noted that for most of Senegal, conditions of discomfort but without danger are observed, while in the northeastern part of Senegal, the category of extreme discomfort prevails. The areas of extreme discomfort extend over the western half of the country during the MAM season, while the eastern half, represented by the east facade, experiences extreme caution or danger conditions in the extreme eastern part of Tambacounda (figure 8b). During the JJA season (figure 8c), extreme discomfort (caution) conditions are observed throughout the country, except in the northeast, particularly in a significant portion of Saint-Louis and Matam, where extreme caution or danger conditions appear. Similar conditions to JJA are observed in the country during the DJF season (figure 8d), but a signal of extreme caution conditions is located in the extreme northeast of Saint-Louis and Matam.

Regarding projected heatwaves in Senegal, the results are presented in figure 8. For the DJF season (figure 8e, i and m), uncomfortable conditions may prevail regardless of the scenario considered, but it remains relatively safe. However, health authorities should remain vigilant as the southeast of Senegal remains under the influence of the category of extreme discomfort. As for the MAM season (figure 8f, j and n), conditions of extreme discomfort, and even danger, extend across the country. During this MAM season, extreme danger conditions are noted in the eastern part of the country, including Matam, Tambacounda, and Kedougou. Moreover, with the scenario ssp585, nearly the entire eastern part of the Podor-Kolda line becomes a high-risk zone. In JJA season (figure 8g, k and o), extreme discomfort conditions, which require caution and may pose potential dangers, affect the central, eastern, and northeastern parts of the country. Lastly, for the SON season (figure 8h, l and p), conditions remain mostly like those observed during DJF season on the country, with a signal of near-extreme danger conditions localized in the northeastern regions of Saint-Louis and Matam.

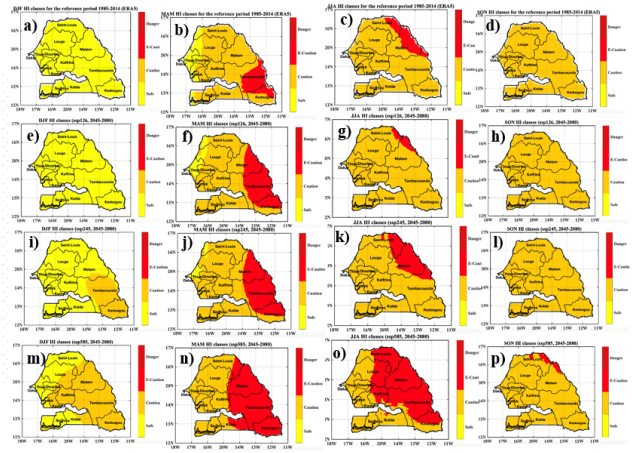

Fig.8. Spatial distribution of seasonal comfort index (CI) class or heat stress categories in Senegal for the reference period (1985-2014) for ERA5 and the projected period (2045-2080). The data pertains to three specific scenarios (SSP126, SSP245, SSP585) originating from the ensemble models of the CMIP6. HI stands for heat index and E-Caution stands for Extreme Caution. DJF=December-January-February; MAM=May-April-May; DJA=June-July-August; SON=September-October-November.

In summary, climate variability and change can impact human health. Whatever the scenario, it is almost certain that global warming will continue, and there is a high probability that the observed increase in heat will impact the climate-sensitive disease. It is very likely that the frequency of extreme heat will increase during the 21st century with an increasing gradient towards southern regions. Senegal faces high climate risks due to mean annual temperatures projected to increase by 1.1 to 3.1°C by the 2060's, and 1.7 to 4.9°C by the 2090's, with projected rates of warming faster in the interior than in those areas closer to the coast; and a greater proportion of precipitation during heavy rainfall events (World Bank. 2020). The mapping of some climate-sensitive diseases in this study and the analysis of risks related to climatic parameters show that the southern regions are mostly exposed vector-borne and water-borne. For insistence, the results indicate that the risk of vector-borne diseases transmission are increase by high increase climate parameters such as rainfall and temperature. Otherwise, a decrease in certain vector-borne diseases such as malaria and dengue fever in certain regions of the country for the far future and for the extreme scenario are highlighted. This could be explained by an extremely hot temperature effect leading to a high mosquito mortality rate. Thus, too hot temperatures could have an impact on the survival pattern of adult mosquitoes starting to kill many adult mosquitoes in impact models and this implies a decrease in the transmission of certain vector-borne diseases such as malaria and dengue fever. However, the preliminary results also show that certain pathologies such as dengue should spread in the south of Senegal in the long term in Ziguinchor and Sedhiou.

Climate change and their impacts on the Senegalese population are aggravating factors of poverty. The Emerging Senegal Plan (PSE) 2035, i.e., the national roadmap for growth, emphasizes the need to reduce the vulnerability of populations to shocks resulting from climate change, making the protection of vulnerable groups one of the pillars of its strategy. Reliable information of this study on expected future climate form the basis for planning and implementing adaptation measures to mitigate the consequences of regional climate change on health sector. The Comfort Index used in this study would be valuable in fields like meteorology, environmental science, and architecture, as it helps in understanding the impact of weather conditions on human well-being and can inform decisions related to building design, urban planning, and outdoor activities.

The main barriers or limits exhibited in the study include the problem of reporting health data and the access to health structures. The access to quality climate data and information in intelligible and usable formats when planning or implementing public health policies constitutes the first barrier to climate change adaptation in Senegal.

AUTHOR CONTRIBUTIONS

Conceptualization, I.D., I.S., J.-A.N. and A.T.G.; methodology, I.D., M.D.; validation, I.S., J.-A.N. and A.T.G.; formal analysis, I.D. and M.D.; investigation, I.D. and M.D.; resources, I.S., J.-A.N. and A.T.G.; writing—original draft preparation, I.D.; writing—review and editing, I.D. and J.-A.N.; supervision, I.S., A.T.G. and J.-A.N.; project administration, A.T.G.; funding acquisition, I.D. and A.T.G. All authors have read and agreed to the published version of the manuscript.

FUNDING

This study, conducted under the auspices of the Senegal National Adaptation Plan support Project-Global Environment Fund (NAP), N° 00109722, Ministry of the Environment and Sustainable Development of Senegal, was made possible by their generous funding. The authors would like to extend their warm thanks to the NAP for their invaluable support.

DATA AVAILABILITY STATEMENT

All relevant data are presented within the manuscript. The WFDEI data are fully available without restriction from: ftp://rfdata:forceDATA@ftp.iiasa.ac.at (accessed on 30 October 2022). Please note that while the bias-corrected CMIP6 data used in this work are available from the LMDz server, the authors of this review do not have the right to publicly share non-open access journal articles.

ACKNOWLEDGMENTS

We thank the United Nations Development (UNDP), N° 5428, who supports the government of Senegal in the development of the NAP-GEF Project, which awarded the achievement of this study. We would like also to thank Gabriel Pierre Diomaye NDIAYE, coordinator of the NAP-GEF project and the institutions from which the authors of this work are affiliated.

CONFLICTS OF INTEREST

The authors declare no conflict of interest. The funders had no role in the design of the study; in the collection, analyses, or interpretation of data; in the writing of the manuscript; or in the decision to publish the results.

REFERENCES

Adhikari S.P., Meng S., Wu Y-J, Mao Y-P., Ye R-X., Wang Q-Z, et al., 2020. Epidemiology, causes, clinical manifestation and diagnosis, prevention, and control of coronavirus disease (COVID-19) during the early outbreak period: a scoping review. *Infect Dis Poverty* ;9: 1–12.

Akaike H., 1974. A new look at the statistical model identification. IEEE Trans. *Autom. Control*. 19: 716–23.

Bhatt S. et al., 2013. The global distribution and burden of dengue. *Nature*, 496(7446), 504-507.

Brady, Oliver J., et al., 2012. Refining the global spatial limits of dengue virus transmission by evidence-based consensus, *PLOS Neglected Tropical Diseases* 6(8): p. e1760.

Chen, N., Zhou, M., Dong, X., Qu, J., Gong, F., Han, Y., ... & Yu, T., 2020. Epidemiological and clinical characteristics of 99 cases of 2019 novel coronavirus pneumonia in Wuhan, China: a descriptive study. *The Lancet*, 395(10223), 507-513.

Cissé, G., R. McLeman, H. Adams, P. Aldunce, K. Bowen, D. Campbell-Lendrum, S. Clayton, K.L. Ebi, J. Hess, C. Huang, Q. Liu, G. McGregor, J. Semenza, and M.C. Tirado, 2022: Health, Wellbeing, and the Changing Structure of Communities. In: Climate Change 2022: Impacts, Adaptation and Vulnerability. Contribution of Working Group II to the Sixth Assessment Report of the Intergovernmental Panel on Climate Change [H.-O. Pörtner, D.C. Roberts, M. Tignor, E.S. Poloczanska, K. Mintenbeck, A. Alegría, M. Craig, S. Langsdorf, S. Löschke, V. Möller, A. Okem, B. Rama (eds.)]. Cambridge University Press, Cambridge, UK and New York, NY, USA, pp. 1041–1170, doi:10.1017/9781009325844.009.

Dee, D. P., Uppala, S. M., Simmons, A. J., Berrisford, P., Poli, P., Kobayashi, S., ... & Vitart, F., 2011. The ERA-Interim reanalysis: configuration and performance of the data assimilation system. *Quart J Roy Meteor Soc* 137: 553–597.

Diouf I., Deme, A., Ndione, J-A., Gaye A.T and Rodriguez-Fonseca, B., 2013. Climat-santé: observation et modélisation du paludisme au Ferlo du

Sénégal. *Comptes rendus. Biologies*, 336(5-6), 253-260.

Diouf I., Fonseca B.F., Deme, A., Caminade C., Morse A.P., Cisse M., Sy, I., Dia I., Ermert V., Ndione J.A. and Gaye A.T., 2017. Comparison of malaria simulations driven by meteorological observations and reanalysis products in Senegal. *International journal of environmental research and public health*, 14(10), p.1119. https://doi.org/10.3390/ijerph14101119.

Diouf I., Rodríguez-Fonseca B.R., Caminade C., Thiaw W.M., Deme A., Morse, A.P., Ndione J.A., Gaye A.T., Diaw A. and Ndiaye M.K.N., 2020. Climate Variability and Malaria over West Africa. *The American Journal of Tropical Medicine and Hygiene*, 102(5),pp.1037-1047. https://doi.org/10.4269/ajtmh.19-0062

Diouf I., Gbenga J.A, Abiodun M.A, Christopher L., Joyce M.S, Pascal Y., Ndione J-A, and Emiola O.G, 2021b. Impact of future climate change on malaria in West Africa, Theoretical and Applied Climatology. vol. 147, no 3, p. 853-865.

Diouf I., Suárez-Moreno R., Rodríguez-Fonseca B., Caminade C., Wade, M., Thiaw M.W, Deme A., Morse, A.P., Ndione J.-A., Gaye A.T, Diaw A., and Ndiaye M.K.N., 2021. Oceanic Influence on Seasonal Malaria Incidence in West Africa. Weather, Climate, and Society. vol. 14, no 1, p. 287-302.

Eyring, V., Bony, S., Meehl, G. A., Senior, C. A., Stevens, B., Stouffer, R. J., and Taylor, K. E, 2016. Overview of the Coupled Model Intercomparison Project Phase 6 (CMIP6) experimental design and organization, *Geosci. Model Dev*., 9, 1937-1958, doi:10.5194/gmd-9-1937-2016.

Ermert, V., A.H. Fink, A.E. Jones, A.P Morse, 2011: Development of a new version of the Liverpool Malaria Model. I. Refining the parameter settings and mathematical formulation of basic processes based on a literature review. *Malar. J*., 10, 35.

Faye M., Dème A., Diongue A. K., & Diouf, I., 2021. Impact of different heat wave definitions on daily mortality in Bandafassi, Senegal. *PloS one*, 16(4), e0249199.

Gao J., Sun Y., Liu Q., Zhou M., Lu Y., Li L., 2015. Impact of extreme high temperature on mortality and regional level definition of heat wave: A multi-city study in China. *Science of the Total Environment* 505, 535–544. pmid:25461056

Gasparrini A., Armstrong B., 2011. The impact of heat waves on mortality. *Epidemiology* 22 (1): 68–73. pmid:21150355

Hastie T.J., Tibshirani RJ., 1990. Generalized Additive Model, London UK: Chapman and Hall.

Hersbach, H.; Bell, B.; Berrisford, P.; Hirahara, S.; Horányi, A.; Muñoz-Sabater, J.; Nicolas, J.; Peubey, C.; Radu, R.; Schepers, D.; et al., 2020. The ERA5 Global Reanalysis. *Q. J. R. Meteorol*. Soc., 146, 1999–2049.

Hoshen, M.B.; Morse, A.P., 2004. A weather-driven model of malaria transmission. *Malar. J.*, 3, 32.

Jeanne I., Rajot J. L., Defossey A., Kairo K. K., Kalache M ., Boisier P., 2005. Dust events and meningitis cases during the dry season (November to April) in the Sahel from 1995 to 2005: methodology for temporal and spatial analysis. *1st international AM M A conference*, 2 December 2005, Dakar, Sénégal.

Lindsay SW, Birley M. H., 1996. Climate change and malaria transmission. Ann Trop Med Parastol; 6:573-88.

Martiny, N., and Chiapello, I., 2013. Assessments for the impact of mineral dust on the meningitis incidence in West Africa. *Atmospheric Environment*, *70*, 245-253.

Michelangeli, P.A., Vrac, M. and Loukos, H., 2009. Probabilistic downscaling approaches: Application to wind cumulative distribution functions. *Geophysical Research Letters*, *36*(11).

Nakazawa, T., & Matsueda, M., 2017. Relationship between meteorological variables/dust and the number of meningitis cases in Burkina Faso. *Meteorological Applications*, 24(3), 423-431.

Nakazawa, T., & Matsueda, M., 2017. Relationship between meteorological variables/dust and the number of meningitis cases in Burkina Faso. *Meteorological Applications*, 24(3), 423-431.

Ndiaye O., Le Hesran J-Y., Etard J-F., Diallo A., Simondon F., Ward M. N., Robert V., 2001. Variations climatiques et mortalité attribuée au paludisme dans la zone de Niakhar, Sénégal, de 1984 à 1996. Cahiers d'études et de recherches francophones / Santé. 2001;11(1):25-33.

Ndione, J. A., Diop, M., Lacaux, J. P., & Gaye, A. T., 2008. Variabilité intra-saisonnière de la pluviométrie et émergence de la fièvre de la vallée du Rift dans la vallée du fleuve Sénégal: nouvelles considérations. *Climatologie*, 5, 83-97.

OMS, 2000 : La fièvre de la vallée du Rift. *Aide-mémoire, 207, Genève*, 1–5.

Petersen E, Koopmans M, Go U, Hamer DH, Petrosillo N, Castelli F, et al., 2020. Comparing SARS-CoV-2 with SARS-CoV and influenza pandemics. *Lancet Infect Dis*. 2020.

Rothfusz, L. P., 1990. The heat index equation (or, more than you ever wanted to know about heat index). Fort Worth, Texas: *National Oceanic and Atmospheric Administration, National Weather Service, Office of Meteorology*, 9023.

Steadman, R. G., 1979. The assessment of sultriness. Part I: A temperature-humidity index based on human physiology and clothing science. Journal of Applied Meteorology, 18(7), 861–873. https://doi.org/10.1175/1520-0450(1979)018%3C0861:TAOSPI%3E2.0.CO;2

Steadman R.G., 1984. A universal scale of apparent temperature. Journal of Climate and Applied *Meteorology*, 23(12), 1674-1687.

Song, Haitao, Dan Tian, and Chunhua Shan, 2020. "Modeling the effect of temperature on dengue virus transmission with periodic delay differential equations." *Mathematical Biosciences and Engineering* 17(4),4147-4164.

Song, H., Tian, D., & Shan, C. (2020). Modeling the effect of temperature on dengue virus transmission with periodic delay differential equations. *Mathematical Biosciences and Engineering*, 17(4), 4147-4164.

Suárez-Moreno, R. and B. Rodríguez-Fonseca, 2015:

S4CAST v2.0: sea surface temperature based statistical seasonal forecast model, *Geosci. Model Dev. Discuss*., 8, 3971-4018, doi:10.5194/gmdd-8-3971-2015

Sylla, M. B., Faye, A., Giorgi, F., Diedhiou, A. and Kunstmann, H., 2018. Projected heat stress under 1.5 C and 2 C global warming scenarios creates unprecedented discomfort for humans in West Africa. *Earth's Future*, 6(7), 1029-1044.

Sy, I., Cissé B., Ndao B., Touré M., Diouf A. A., Sarr M. A., Ndiaye O., Ndiaye Y., Badiane D., Lalou R., Janicot S., Ndione J-A., 2022. Heat waves and health risks in the northern part of Senegal: analysing the distribution of temperature-related diseases and associated risk factors. *Environ Sci Pollut Res* (2022). https://doi.org/10.1007/s11356-022-21205-x

Trape J-F, 1999. Changements climatiques et maladies infectieuses : le cas du paludisme et de la borréliose à tiques. Med Mal Infect 1999 ; 29 : 296-300

Trisos, C.H., I.O. Adelekan, E. Totin, A. Ayanlade, J. Efitre, A. Gemeda, K. Kalaba, C. Lennard, C. Masao, Y. Mgaya, G. Ngaruiya, D. Olago, N.P. Simpson, and S. Zakieldeen, 2022: Africa. In: Climate Change 2022: Impacts, Adaptation and Vulnerability. Contribution of Working Group II to the Sixth Assessment Report of the Intergovernmental Panel on Climate Change [H.-O. Pörtner, D.C. Roberts, M. Tignor, E.S. Poloczanska, K. Mintenbeck, A. Alegría, M. Craig, S. Langsdorf, S. Löschke, V. Möller, A. Okem, B. Rama (eds.)]. Cambridge University Press, Cambridge, UK and New York, NY, USA, pp. 1285–1455, doi:10.1017/9781009325844.011.

World Bank. 2020. Senegal climate data projections. https://climateknowledgeportal.worldbank.org/country/senegal/climate-data-projections.

Zhongming, Zhu, et al. 2021. AR6 Climate Change 2021: The Physical Science Basis.